

Tunable Multifocal THz Metalens Based on Metal-Insulator Transition of VO₂ Film

Roya Kargar¹, Kasra Rouhi¹, and Ali Abdolali^{1*}

¹Applied Electromagnetic Laboratory, School of Electrical Engineering, Iran University of Science and Technology, Tehran, 1684613114, Iran

*Corresponding author. E-mail: abdolali@iust.ac.ir (Ali Abdolali)

Abstract – Recently, metalenses which consist of metasurface arrays, have attracted attention due to their more condensed size in comparison with conventional lenses. In this paper, we propose a reconfigurable coding metasurface hybridized with vanadium dioxide (VO₂) for wavefront manipulation at terahertz (THz) frequencies. At room temperature, the unit-cell can reflect as a "1" bit under linearly y polarized illuminated waves. Besides, when the temperature is increased, VO₂ would be in a fully metallic state; therefore, unit-cell can act as a "0" reflection phase. Furthermore, by changing the unit-cells arrangements on a metalens surface, the proposed device can focus the incident beam at any position according to a particular design. Numerical simulations demonstrate that the designed VO₂-assisted metasurface can generate one and multi-focal spot in reflection mode as expected. Also, theoretical results depict an excellent agreement with obtained simulation results. The presented metalens has notable potential in THz high-resolution imaging and optical coding.

I. Introduction

Metasurfaces, the two-dimensional version of metamaterials, have recently attracted significant consideration due to their ability to manipulate arbitrary electromagnetic wavefronts by adding extraordinary field discontinuities over the interface [1,2]. Planar equivalents of conventional bulky optical devices such as lenses [3,4], holograms [5,6], absorbers [7,8], optical signal processors [9], beam deflectors [10–12], polarizers [13], and so on have been experimentally demonstrated in different electromagnetic frequencies. These devices consist of a subwavelength element arranged on a two-dimensional surface with a specific order. Indeed metasurfaces are mimicking the phase profile of the typical bulk optical devices. Such metasurface-based flat devices represent a new class of optical and THz components that are compact and lightweight. Although metasurface application and fabrication methods improved

in recent years but reconfigurable metasurface devices are a significant missing link in modern pragmatic devices and systems.

Mostly metasurfaces are composed of passive building blocks that cause a lack of tunability and reconfigurability of response. Therefore, one metasurface-based device only grants one or a few functions that are inherently limiting their practical impact. Among these devices, compact lenses with reconfigurable focal points have various applications. Hence, various methods have been developed to make such devices. Deformable solid and liquid-filled lenses with mechanical [14], electrowetting [15,16], electromechanical [17], and thermal tuning [18] mechanisms have been proposed in several pieces of research. These devices are more compact than conventional varifocal lenses and have different tuning rates ranging from few Hz to a few hundreds of Hz. On the contrary, liquid crystal lenses with a tunable focus spot have higher tuning speeds, but they suffer from polarization dependence and limited tuning range [19,20]. Freeform optical elements that can tune the focus distance upon lateral displacement of the components have also been expressed [21]. These devices are based on the mechanical movement of massive elements and are consequently not very compact nor fast. Highly tunable elastic dielectric metasurface lenses based on stretchable substrates have also been proved, but they have low speeds and require a radial stretching mechanism that might increase the device size [22,23]. Also, controlling the axial movement or angular orientation of the metalens via integrating with the microelectromechanical systems [24,25] and laterally actuating two separate cubic metasurfaces based on the Alvarez lens design [26] are novel approaches for tunable metalens. On the other side, procedures of including tunable materials into metasurfaces for changing the functionality, such as the use of liquid crystals [27], phase-change materials [28,29], graphene [30–32] or others are widespread in various devices. Dynamic responses of these materials enable active THz materials that are excited by external stimuli via photoexcitation, electric or magnetic bias and temperature.

Vanadium dioxide is an advantageous material to accomplish a switchable performance in electromagnetic devices. VO₂ is praised for its phase transition feature, which changes the material from a semiconductor to a metallic state at a critical temperature $T_c = 68^\circ\text{C}$. This unique characteristic is due to physical and structural variations, which make changes in the material electromagnetic properties [33]. Atomic-level deformation in phase change materials has capable of offering drastic variations in material properties over a broad spectral range during the phase transition. These features make VO₂ a promising phase-change material to be utilized in tunable metasurfaces. By designing sub-wavelength structures, VO₂ has been employed to fabricate tunable meta-devices working at THz and other optical frequencies. The

dielectric properties of VO₂ could be impressed by thermal, electrical, optical, and mechanical stimuli, and the substantial point in this process is reversible and has a hysteresis associated characteristic [34]. Recently VO₂-assisted metasurfaces attract scientist's attention and utilized in a diverse application for electromagnetic wave manipulation [35–37].

In this manuscript, we propose a high-performance, one-bit tunable metasurface by utilizing VO₂ film for the THz applications. According to the theory of fuzzy quantification, two dynamically switchable metasurfaces whose reflection phases can possess both of 0 and π values, are utilized as “0” and “1” building blocks of 1-bit coding metasurface. By adjusting the vanadium dioxide temperature in each unit cell and implementing the required reflection profile for wave concentration, an exact focus point is obtained at an arbitrary focal point. The results illustrate that the proposed THz metalens exhibits precise focusing at a frequency of 1.6 THz, and it can include the whole half-space. Also, this structure has a valuable capability to concentrate reflected waves in more than one focus region. In the following subsections, we will describe our proposed one-bit digital metasurface and provide the required mathematical calculations and analysis to utilize VO₂-assisted metasurface as multifocal metalens. We have investigated all simulation results by full-wave simulation software and compared them with a theoretical approach.

II. Vanadium Dioxide

Vanadium dioxide is known for exhibiting a reversible first-order phase transition from a monoclinic to a tetragonal crystalline structure at a transition temperature of 68 °C. Owing to its association with a strong variation of both the resistivity and the optical dielectric constant, this solid phase transition attracts substantial interest. VO₂ is transparent at infrared frequency range at the insulator phase, while VO₂ at the metallic phase is opaque at the most spectral frequencies. Due to its low photon energy, THz radiation is sensitive to the change of free carrier density in a phase transition [38].

Another VO₂ property is its sub-picosecond time duration over which the solid phase transition occurs. All these characteristics make VO₂ extremely interesting not only for the fundamental understanding of the physics of this semiconductor to metal transition but also for near room temperature switching devices. As mentioned in other references, the electrical resistance of the VO₂ films is a function of temperature for both heating and cooling cycles. This cycle is not unique for the heating and cooling processes in transition temperature. The metal-insulator transition behavior of VO₂ films makes it as two dissimilar materials in which one of them is an insulator, and the other one is metal. Its relative permittivity is about 9 in the

insulating state, while the conductivity is smaller than 200 S/m. When VO₂ passes the transition temperature, it comes to the metallic state. In this case, relative permittivity is constant, but the conductivity increases as high as an order of 10⁵ [39].

III. Metasurface Structure

Hereby we introduce VO₂ in a suitably configured structure such that its reflection phase is either 0° or 180° depending on the state of VO₂. Based on arrays of such a metasurface, we demonstrate dynamic electric field distribution at the operating frequency of 1.6 THz from rigorous full-wave simulations. The proposed metasurface consists of three layers of gold, silicon, and combination of VO₂ and gold, respectively, from bottom to top. Each unit cell consists of three gold fragments with a thickness of $t_m=200$ nm. Also, we have incorporated four similar VO₂ fragments into the gold gaps, which can be programmed individually. The spacer dielectric substrate is lossy silicon, which has the relative permittivity of $\epsilon_r=11.9$ and $\delta=0.00025$. Finally, a gold ground plane has been embedded in the last layer to prevent electromagnetic radiation transmissions. *Figure 1* illustrates a schematic of a designed unit cell and all the required geometry parameters. The reprogrammable device can be employed to deliver the desired bias voltages at its output and control each meta-atom temperature to set the operational status of each coding element, individually. Consequently, by a real-time switch between arbitrary coding patterns, a different focal spot can be achieved.

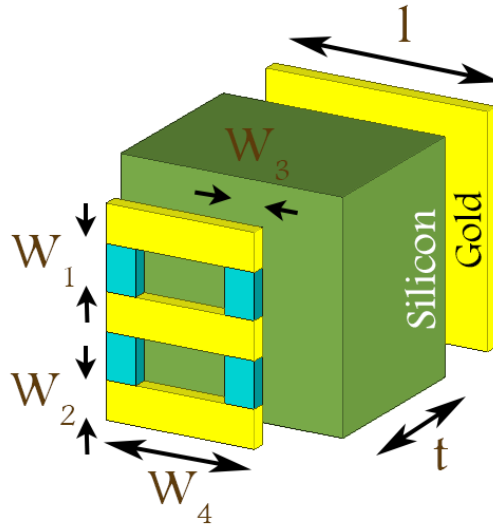


Figure 1. The schematic of the proposed unit cell and constituent materials have been depicted in this figure.

The yellow material is gold, the green material depict lossy silicon, and the blue material is VO₂ in both insulator and lossy metal state. In the proposed structure, $w_1=3 \mu\text{m}$, $w_2=2.5 \mu\text{m}$, $w_3=2 \mu\text{m}$, $w_4=10 \mu\text{m}$, $l=15 \mu\text{m}$, $t=12 \mu\text{m}$.

All the designs are carried out using CST Microwave Studio with the frequency-domain solver to extract the reflection phases and amplitude coefficients for an infinite array of “0” and “1” coding elements. To simulate the suggested structure, periodic boundary conditions are applied in the x and y directions to consider the mutual coupling influence between adjoining elements. Also, the Floquet ports are assigned to the z-direction to illuminate incident y-polarized waves. In metalens design, the conductivity of VO2 in each unit cell is varied to tailor the required phase change, while the construction of the whole metasurface is kept constant. When VO2 is insulating, an element is coded by “1” and correspondingly, an element with VO2 in the metal state is coded by ”0”.

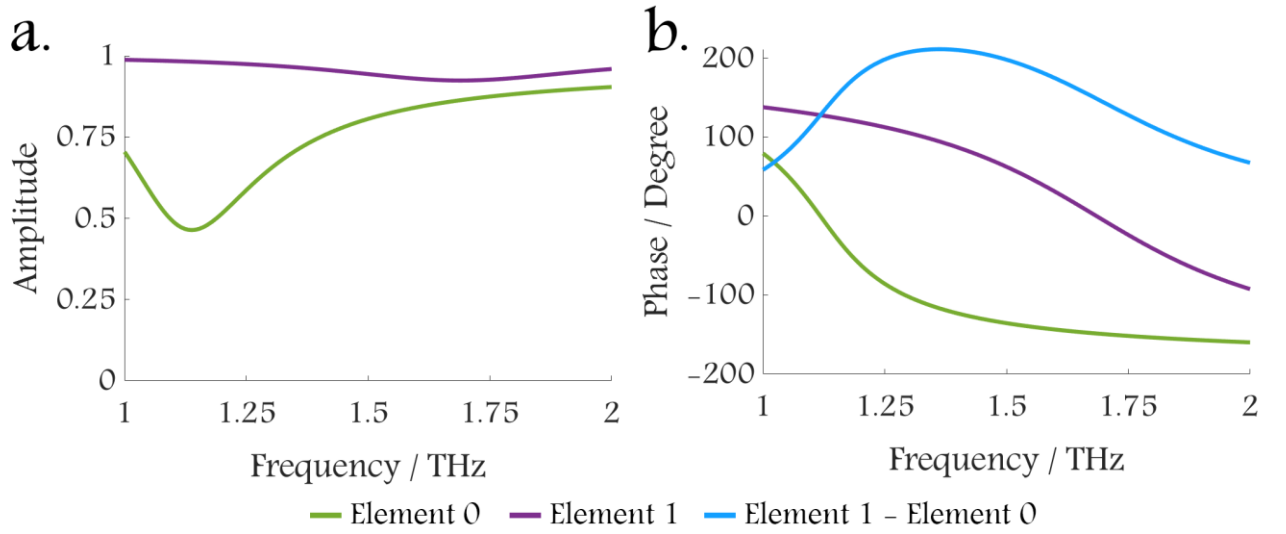


Figure 2. Reflection coefficient response of the (a) amplitude and (b) phase of reconfigurable digital meta-atom under y-polarization illumination from 1 to 2 THz. According to extracted results from simulation, 1.6 THz selected as a primary working frequency.

IV. The Focusing Properties of Tunable Metalens Structure

To demonstrate how VO2-assisted unit cells are utilized in metasurface designs for manipulating the scattered field concentration dynamically, we first describe the required phase distribution for beam concentration. The waves reflected from the metasurface must constructively interfere at the focal point similar to the waves that are transmitted from a conventional lens. To construct a planar lens, we spatially distribute the coding unit cell with varying reflection phase to realize the hyperbolic phase profile. The target phase profile of the metalens is given by the following expression [40]:

$$\varphi_{ref}(x, y) = k\sqrt{(x - x_{foc})^2 + (y - y_{foc})^2 + z_{foc}^2} - z_{foc} \quad (1)$$

Where $k=2\pi/\lambda$ is the wave vector in desired frequency, $A(x,y,0)$ is a point on the metasurface, and $A'(x_{foc},y_{foc},z_{foc})$ is a predetermined focal point in half-space. In this equation, we assume

that the metalens is positioned at the $z=0$ plane, and the center of each unit cell represents the element location.

V. Focus Results

In this section, we will investigate our structure capability to concentrate reflected beam in a predetermined focal spot. In the first example, phase-change reconfigurable metasurface designed to concentrate radiated waves at the metasurface normal axis. Indeed we have started to arrange digital building block in origin of coordinates and utilized required parabolic phase distribution. *Figure 3 (a)* shows a metasurface phase profile to concentrate the beam at $x=0 \mu\text{m}$, $y=0 \mu\text{m}$, $z=170 \mu\text{m}$. This structure composed of 80×80 elements, which is equal to $6.4\lambda \times 6.4\lambda$ at 1.6 THz approximately. Obtained results for electric field distribution have been demonstrated in *Figure 4 (a-c)*. As we can see in these figures, the metasurface produces efficient electric field concentration very close to the desired point. As exhibited in *Figure 4 (a),(b)*, side lobes appear around the focal spot due to the finite and discrete nature of the proposed metasurface. Side lobes level value and focal point position accuracy can be improved with larger metasurfaces size or smaller unit cell dimension. To evaluate simulation results, we have utilized a theoretical approach to calculate the electric field distribution; then, we have compared theoretical and simulation results.

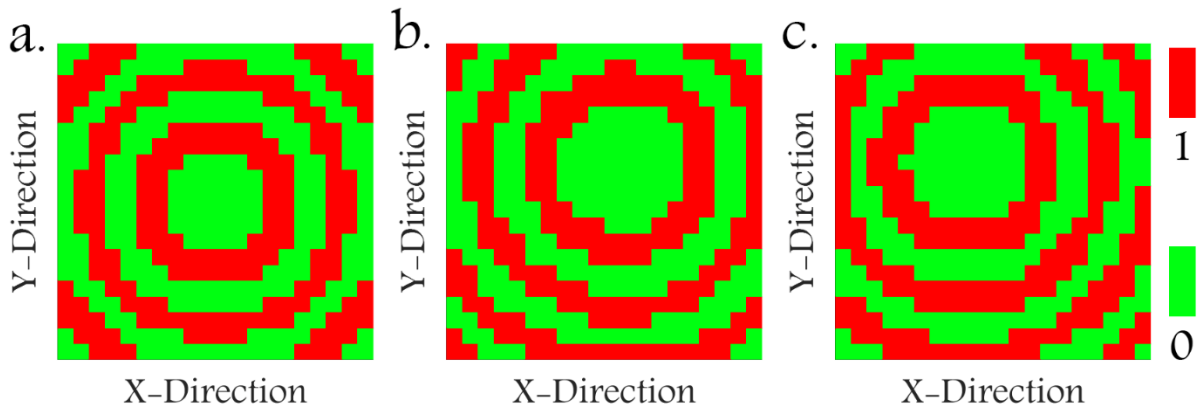


Figure 3. Encoded unit cells arrangement used to achieve the focal spot at (a) $x=0 \mu\text{m}$, $y=0 \mu\text{m}$, $z=170 \mu\text{m}$ (b) $x=70 \mu\text{m}$, $y=140 \mu\text{m}$, $z=270 \mu\text{m}$ (c) $x=-100 \mu\text{m}$, $y=155 \mu\text{m}$, $z=230 \mu\text{m}$.

According to the Huygens' principle, each radiative elements can be assumed as a secondary source, so the meta-atoms are equivalent to a point sources. It gives rise to a diffraction effect at the rear surface of the structure. Due to the particular phase distribution of structure, the effect could be equivalent to the combined effect of a zone plate and an echelle grating [41]. To confirm our analysis, we departed from the Fresnel diffraction method to look through the electric field distribution [6]

$$E(r_1) = \iint E(r_0) \frac{-jz \exp(-jkd_{01})}{\lambda d_{01}^2} ds \quad (2)$$

Where $E(r_1)$ demonstrates the electric field at point r_1 on the observation point, $E(r_0) = U_{m,n} \exp(j\varphi_{m,n})$ is the electric field at point r_0 on the metasurface, whereas this reflection distribution is equivalent to reflection amplitude and phase profile, z is a distance between metasurface and observation point, and d_{01} is the distance between points r_0 and r_1 . Also, according to the digitalized nature of the structure, we can rewrite Fresnel diffraction as below:

$$E(r_1) = \sum_M \sum_N U_{m,n} \exp(j\varphi_{m,n}) \frac{-jz \exp(-jkd_{01})}{\lambda d_{01}^2} \quad (3)$$

The calculated result by utilizing the analytical approach is shown by the green dashed lines in **Figures 4 (a-c)**, which agrees well with the solid purple lines obtained by simulation. For assurance of the meta-device dynamic response, two more examples with different focusing spots were presented, which demonstrate that the focal point can be switched in a real-time manner in the whole space. As a second example, we have selected a focal point far from the normal axis. We have arranged a phase profile according to **Figure 3 (b)** to concentrate reflected beam at $x=70 \mu\text{m}$, $y=140 \mu\text{m}$, and $z=270 \mu\text{m}$. The simulation and analytical results have been shown in **Figures 4 (d-f)**. The simulated phase profile exhibits a proposed device capability to concentrate reflected energy in a different spot out of the normal axis. The whole space scanning capability is the most significant feature of reconfigurable metalens for imaging applications, whereas in the conventional imaging systems scanning has been done by using mechanical movements [25]. Indeed in the VO₂-assisted metalens, mechanical tunability replaced by temperature tunability via electrical stimulation. Finally, in the last example, we have examined the surface tunability to concentrate reflected beam at $x=-100 \mu\text{m}$, $y=155 \mu\text{m}$, and $z=230 \mu\text{m}$. The required encoded phase profile and one-dimensional electric field distribution exhibited in **Figure 3 (c)** and **Figures 4 (g-i)**, respectively, which we can observe a good agreement between theoretical and simulation results.

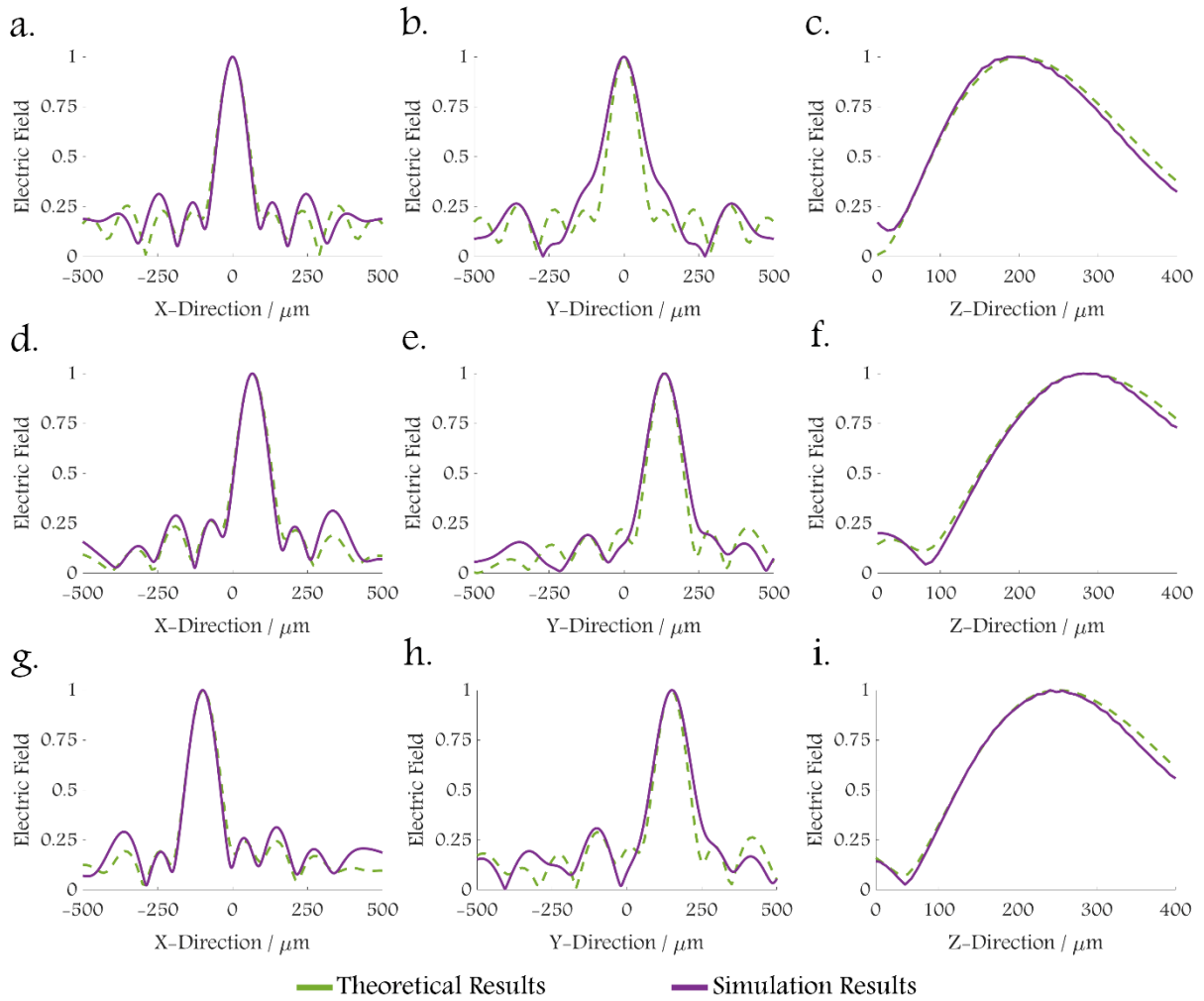


Figure 4. One-dimensional electric field distributions of VO₂-assisted metalens with the different focusing spot at the working frequency of 1.6 THz in three directions. All figures contain theoretical and simulation results. (a-c) $x=0 \mu\text{m}$, $y=0 \mu\text{m}$, $z=170 \mu\text{m}$ (d-f) $x=70 \mu\text{m}$, $y=140 \mu\text{m}$, $z=270 \mu\text{m}$ (g-i) $x=-100 \mu\text{m}$, $y=155 \mu\text{m}$, $z=230 \mu\text{m}$.

VI. Multiple Focus Results

Proposed VO₂-assisted metasurface has a valuable feature to concentrate reflected beam at more than one focal spot. To examine this capability, we have divided a structure to multi sections that each section produces one focal point in space. Different distribution of digital elements in each segment leads to multiple focal points only by one planar structure. [Figure 5](#) illustrates the schematic diagram for a suggested approach to generate two focal spots in different positions, simultaneously.

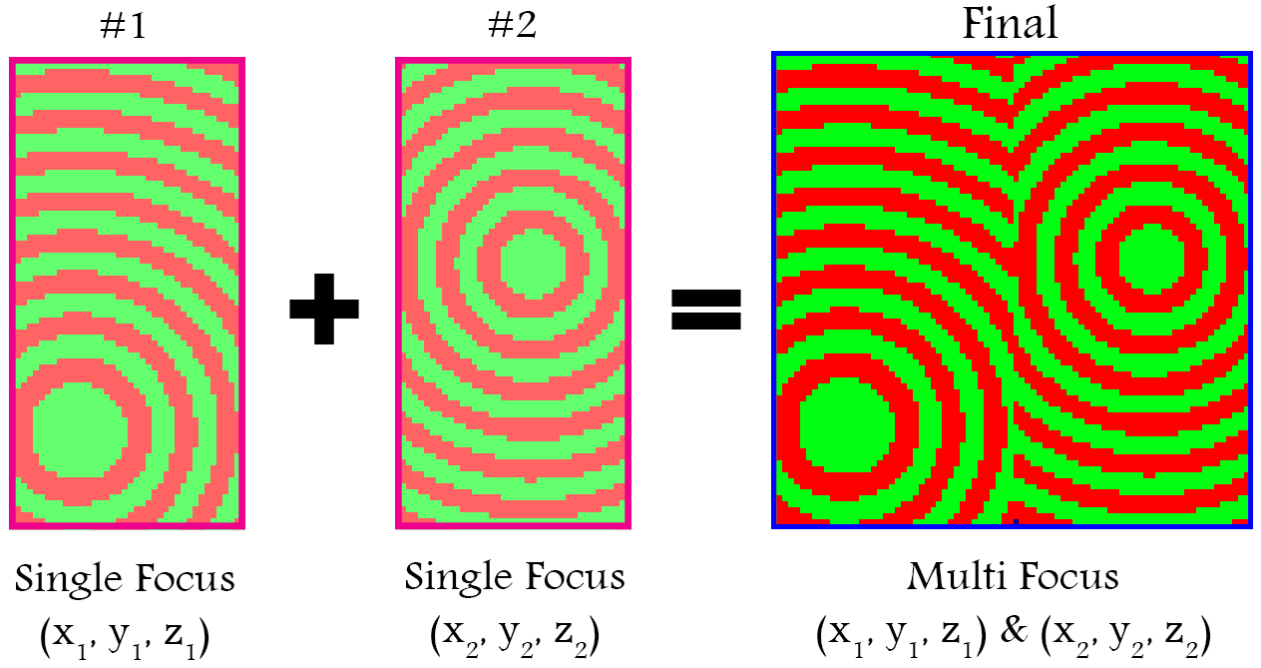


Figure 5. Schematic diagram of multifocal metasurface by using dividing approach.

For instance, we have calculated required encoded arrangement to concentrate reflected beam at $x=-105 \mu\text{m}$, $y=285 \mu\text{m}$, and $z=100 \mu\text{m}$ for the first section and $x=185 \mu\text{m}$, $y=-150 \mu\text{m}$, and $z=100 \mu\text{m}$ for the second section. **Figure 6 (a)** exhibits simulation result in the focal plane, and **Figure 6 (b)** shows the analytical result for this example. In this example, selected focal points are placed in the same plane and have a similar distance with metasurface, but it is possible to concentrate reflected energy in two different planes.

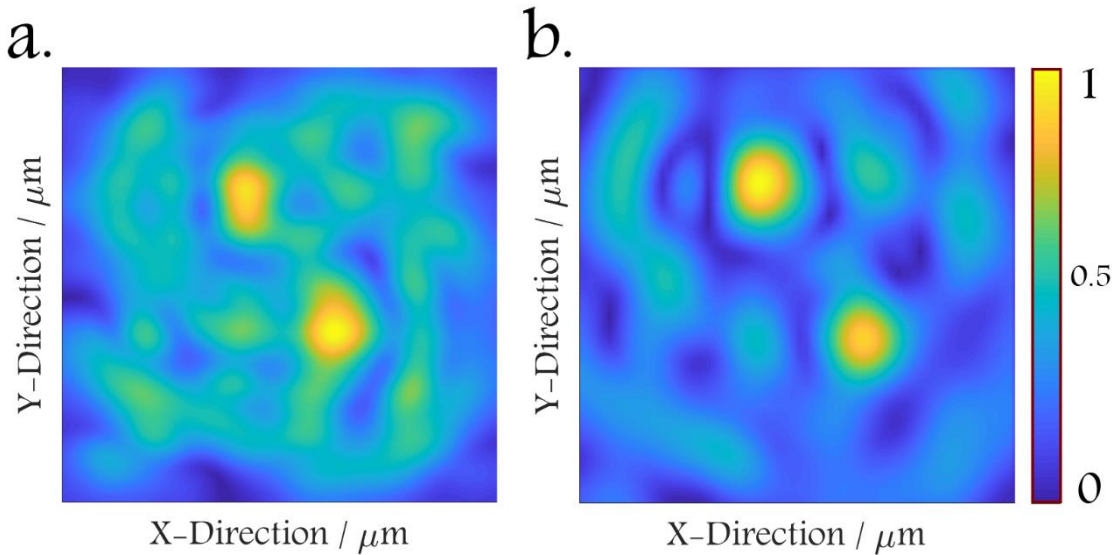


Figure 6. Two-dimensional electric field distribution of VO₂-assisted metalens for multifocal application at a frequency of 1.6 THz in similar transverse focal plane $z=100 \mu\text{m}$. These figures contain obtained results by (a) simulation and (b) theoretical approach.

VII. Conclusion

In summary, we have proposed an engineered VO₂-assisted metalens for dynamic THz wave concentration. Designed unit cell has a particular capability to tune between two digital states, “0” and “1” by controlling VO₂ material temperature. Based on this configuration, a THz metalens with tunable focal point is designed and numerically demonstrated. Besides, we have proposed a dividing method to generate multifocal metalens and examine this method by a numerical and analytical approach. The proposed design and concept have the flexibility to be developed for more than two focal points with high-resolution concentration. The designed VO₂-assisted metasurface has excellent potentials for tunable, multifunctional, and integrated THz devices.

REFERENCES

- [1] T. Liu, Q. Liu, S. Yang, Z. Jiang, T. Wang, X. Yang, Shaping a far-field optical needle by a regular nanostructured metasurface, *Opt. Commun.* (2017). doi:10.1016/j.optcom.2017.02.031.
- [2] H. Barati, M.H. Fakheri, A. Abdolali, Exploiting transformation optics for arbitrary manipulation of antenna radiation pattern, *IET Microwaves, Antennas Propag.* (2019). doi:10.1049/iet-map.2018.5207.
- [3] M. Khorasaninejad, W.T. Chen, R.C. Devlin, J. Oh, A.Y. Zhu, F. Capasso, Metalenses at visible wavelengths: Diffraction-limited focusing and subwavelength resolution imaging, *Science* (80-). (2016). doi:10.1126/science.aaf6644.
- [4] H. Zhao, Z. Chen, F. Su, G. Ren, F. Liu, J. Yao, Terahertz wavefront manipulating by double-layer graphene ribbons metasurface, *Opt. Commun.* 402 (2017) 523–526. doi:10.1016/j.optcom.2017.06.044.
- [5] A.U.R. Khalid, J. Liu, Y. Han, N. Ullah, R. Zhao, Y. Wang, Multichannel polarization encoded reflective metahologram using VO₂ spacer in visible regime, *Opt. Commun.* (2019). doi:10.1016/j.optcom.2019.06.048.
- [6] Q. Wang, X. Zhang, Y. Xu, J. Gu, Y. Li, Z. Tian, R. Singh, S. Zhang, J. Han, W. Zhang, Broadband metasurface holograms: Toward complete phase and amplitude engineering, *Sci. Rep.* (2016). doi:10.1038/srep32867.
- [7] M. Chen, W. Sun, J. Cai, L. Chang, X. Xiao, Frequency-tunable terahertz absorbers based on graphene metasurface, *Opt. Commun.* (2017). doi:10.1016/j.optcom.2016.07.077.
- [8] M. Rahmzadeh, H. Rajabalipanah, A. Abdolali, Multilayer graphene-based metasurfaces: robust design method for extremely broadband, wide-angle, and polarization-insensitive terahertz absorbers, *Appl. Opt.* (2018). doi:10.1364/ao.57.000959.
- [9] A. Momeni, H. Rajabalipanah, A. Abdolali, K. Achouri, Generalized Optical Signal Processing Based on Multioperator Metasurfaces Synthesized by Susceptibility Tensors, *Phys. Rev. Appl.* 11 (2019) 064042.
- [10] Q. Zhang, M. Li, T. Liao, X. Cui, Design of beam deflector, splitters, wave plates and metalens using photonic elements with dielectric metasurface, *Opt. Commun.* (2018). doi:10.1016/j.optcom.2017.11.011.
- [11] S.E. Hosseininejad, K. Rouhi, M. Neshat, A. Cabellos-Aparicio, S. Abadal, E. Alarcón, Digital Metasurface Based on Graphene: An Application to Beam Steering in Terahertz Plasmonic Antennas, *IEEE Trans. Nanotechnol.* (2019). doi:10.1109/TNANO.2019.2923727.
- [12] J. Wang, Y. Jiang, Gradient metasurface for four-direction anomalous reflection in terahertz, *Opt. Commun.* 416 (2018) 125–129. doi:10.1016/j.optcom.2018.01.045.
- [13] C. Wang, W. Liu, Z. Li, H. Cheng, Z. Li, S. Chen, J. Tian, Dynamically Tunable Deep Subwavelength High-Order Anomalous Reflection Using Graphene Metasurfaces, *Adv. Opt. Mater.* 6 (2018) 1–7. doi:10.1002/adom.201701047.
- [14] K.H. Jeong, G.L. Lin, N. Chronis, L.P. Lee, Tunable microdoublet lens array, in: *Proc. IEEE Int. Conf. Micro Electro Mech. Syst.*, 2004. doi:10.1109/MEMSYS.2003.1189681.
- [15] L. Li, D. Wang, C. Liu, Q.-H. Wang, Zoom microscope objective using electrowetting lenses, *Opt. Express.* (2016). doi:10.1364/oe.24.002931.
- [16] N.R. Smith, L. Hou, J. Zhang, J. Heikenfeld, Fabrication and demonstration of electrowetting liquid lens arrays, *IEEE/OSA J. Disp. Technol.* (2009). doi:10.1109/JDT.2009.2027036.

- [17] S. Shian, R.M. Diebold, D.R. Clarke, Tunable lenses using transparent dielectric elastomer actuators, *Opt. Express*. (2013). doi:10.1364/oe.21.008669.
- [18] K. Dobek, Motionless microscopy with tunable thermal lens, *Opt. Express*. (2018). doi:10.1364/oe.26.003892.
- [19] O. Pishnyak, S. Sato, O.D. Lavrentovich, Electrically tunable lens based on a dual-frequency nematic liquid crystal, *Appl. Opt.* (2006). doi:10.1364/ao.45.004576.
- [20] H. Ren, Y.H. Fan, S. Gauza, S.T. Wu, Tunable-focus flat liquid crystal spherical lens, *Appl. Phys. Lett.* (2004). doi:10.1063/1.1760226.
- [21] A. Zhan, S. Colburn, C.M. Dodson, A. Majumdar, Metasurface Freeform Nanophotonics, *Sci. Rep.* (2017). doi:10.1038/s41598-017-01908-9.
- [22] S.M. Kamali, E. Arbabi, A. Arbabi, Y. Horie, A. Faraon, Highly tunable elastic dielectric metasurface lenses, *Laser Photonics Rev.* (2016). doi:10.1002/lpor.201600144.
- [23] H.S. Ee, R. Agarwal, Tunable Metasurface and Flat Optical Zoom Lens on a Stretchable Substrate, *Nano Lett.* (2016). doi:10.1021/acs.nanolett.6b00618.
- [24] E. Arbabi, A. Arbabi, S.M. Kamali, Y. Horie, M.S. Faraji-Dana, A. Faraon, MEMS-tunable dielectric metasurface lens, *Nat. Commun.* (2018). doi:10.1038/s41467-018-03155-6.
- [25] T. Roy, S. Zhang, I.W. Jung, M. Troccoli, F. Capasso, D. Lopez, Dynamic metasurface lens based on MEMS technology, *APL Photonics*. (2018). doi:10.1063/1.5018865.
- [26] S. Colburn, A. Zhan, A. Majumdar, Varifocal zoom imaging with large area focal length adjustable metalenses, *Optica*. (2018). doi:10.1364/optica.5.000825.
- [27] Z. Nasehi, N. Nozhat, Liquid crystal based tunable plasmonic subtractive color filters, *Opt. Commun.* 445 (2019) 96–100. doi:10.1016/j.optcom.2019.04.012.
- [28] E.T. Hu, T. Gu, S. Guo, K.Y. Zang, H.T. Tu, K.H. Yu, W. Wei, Y.X. Zheng, S.Y. Wang, R.J. Zhang, Y.P. Lee, L.Y. Chen, Tunable broadband near-infrared absorber based on ultrathin phase-change material, *Opt. Commun.* (2017). doi:10.1016/j.optcom.2017.07.027.
- [29] F. Ding, Y. Yang, S.I. Bozhevolnyi, Dynamic Metasurfaces Using Phase-Change Chalcogenides, *Adv. Opt. Mater.* (2019). doi:10.1002/adom.201801709.
- [30] K. Rouhi, H. Rajabalipanah, A. Abdolali, Multi-bit graphene-based bias-encoded metasurfaces for real-time terahertz wavefront shaping: From controllable orbital angular momentum generation toward arbitrary beam tailoring, *Carbon* N. Y. 149 (2019) 125–138. doi:10.1016/j.carbon.2019.04.034.
- [31] K. Rouhi, H. Rajabalipanah, A. Abdolali, Real-Time and Broadband Terahertz Wave Scattering Manipulation via Polarization-Insensitive Conformal Graphene-Based Coding Metasurfaces, *Ann. Phys.* 1700310 (2017) 1–9. doi:10.1002/andp.201700310.
- [32] A. Momeni, K. Rouhi, H. Rajabalipanah, A. Abdolali, An Information Theory-Inspired Strategy for Design of Re-programmable Encrypted Graphene-based Coding Metasurfaces at Terahertz Frequencies, *Sci. Rep.* 8 (2018) 6200. doi:10.1038/s41598-018-24553-2.
- [33] A.S. Barker, H.W. Verleur, H.J. Guggenheim, Infrared optical properties of vanadium dioxide above and below the transition temperature, *Phys. Rev. Lett.* (1966). doi:10.1103/PhysRevLett.17.1286.
- [34] J. Narayan, V.M. Bhosle, Phase transition and critical issues in structure-property correlations of vanadium oxide, *J. Appl. Phys.* (2006). doi:10.1063/1.2384798.
- [35] H. Liu, Y.X. Fan, H.G. Chen, L. Li, Z.Y. Tao, Active tunable terahertz resonators based on

- hybrid vanadium oxide metasurface, *Opt. Commun.* (2019). doi:10.1016/j.optcom.2019.04.054.
- [36] F. Hu, Q. Rong, Y. Zhou, T. Li, W. Zhang, S. Yin, Y. Chen, J. Han, G. Jiang, P. Zhu, Y. Chen, Terahertz intensity modulator based on low current controlled vanadium dioxide composite metamaterial, *Opt. Commun.* (2019). doi:10.1016/j.optcom.2019.02.032.
- [37] J. Bai, S. Zhang, F. Fan, S. Wang, X. Sun, Y. Miao, S. Chang, Tunable broadband THz absorber using vanadium dioxide metamaterials, *Opt. Commun.* (2019).
- [38] B. Wu, M. Zhao, J. Zhou, X. Xu, C. Wang, Numerical investigation of nonlinear photothermal effect in Vanadium Dioxide phase-change particles, *Opt. Commun.* (2018). doi:10.1016/j.optcom.2018.06.049.
- [39] F. Ding, S. Zhong, S.I. Bozhevolnyi, Vanadium Dioxide Integrated Metasurfaces with Switchable Functionalities at Terahertz Frequencies, *Adv. Opt. Mater.* 6 (2018) 1–8. doi:10.1002/adom.201701204.
- [40] S.E. Hosseini, K. Rouhi, M. Neshat, A. Cabellos-Aparicio, S. Abadal, E. Alarcón, Reprogrammable Metasurface Based on Graphene for THz Imaging: Flat Metamirror with Adaptive Focal Point, *Sci. Rep.* 9 (2019) 2868. doi:10.1038/s41598-019-39266-3.
- [41] Q. Yang, J. Gu, D. Wang, X. Zhang, Z. Tian, C. Ouyang, R. Singh, J. Han, W. Zhang, Efficient flat metasurface lens for terahertz imaging, *Opt. Express.* (2014). doi:10.1364/oe.22.025931.